

## Lattice dynamics of nickel

Natthi Singh, Joginder Singh, and Satya Prakash

Department of Physics, Panjab University, Chandigarh-160014, India

(Received 3 December 1974)

The phonon frequencies of nickel are investigated using a unified approach of lattice dynamics. The inversion of the dielectric matrix is carried out using the *Ansatz* due to Sinha *et al.* and is evaluated in the noninteracting band scheme. The bare ion potential is replaced by the Harrison simple-metal pseudopotential and Animalu's transition-metal model potential. The calculated phonon frequencies are found in reasonably good agreement with the experimental values for the paramagnetic and the ferromagnetic phases.

### I. INTRODUCTION

The problem of lattice dynamics of transition metals is interesting but characteristically difficult. In these metals the distinction between the core and the conduction electrons is not clear. The outermost  $d$  shell is not completely filled, and the electronic band-structure calculations show that the wave functions of the conduction electrons have  $s$  character as well as  $d$  character.<sup>1</sup> The  $d$  electrons are neither tightly bound to the core nor totally free. Harrison analyzed this problem by generalizing the pseudopotential theory<sup>2</sup> which was extended and used by Moriarty<sup>3</sup> for the calculation of phonon frequencies and cohesive energies of noble and alkaline-earth metals. Panitz, Cutler, and King<sup>4</sup> have also applied this formalism to calculate the phonon spectra of zinc. However, an explicit calculation for a partially filled  $d$ -band metal is not yet carried out using this approach. Sinha<sup>5</sup> and Golibersuch<sup>6</sup> have also studied the electron-phonon interaction in transition metals using the augmented-plane-wave method.

Earlier Prakash and Joshi<sup>7</sup> suggested a noninteracting band scheme and calculated the phonon frequencies of nickel and copper. The scheme was further extended by Singh and Prakash<sup>8</sup> to calculate the phonon frequencies and cohesive energies of all the noble metals. In these calculations only the diagonal part of the dielectric matrix was included. Hanke<sup>9</sup> extended the calculations for paramagnetic nickel and included the diagonal and nondiagonal parts for the  $d$ - $d$  intraband transitions which give rise to the dipolar model of lattice dynamics of transition metals. However, Hanke neglected the diagonal and nondiagonal parts of the dielectric matrix for  $d$ - $s$  and  $s$ - $d$  interband transitions. The contribution of these transitions was found to be small for paramagnetic nickel, but this may be a leading term in other transition metals such as chromium.<sup>10</sup> Recently the authors have explicitly calculated the diagonal and nondiagonal parts of the dielectric matrix in the noninteracting-spin band scheme for ferromagnetic and paramagnetic phases of nickel<sup>11</sup> (hereafter this paper will be referred to

as I). In the present paper we have made an attempt to include the complete dielectric matrix in the calculation of phonon frequencies of transition metals. The inversion of the dielectric matrix is carried out using the factorization *Ansatz* due to Sinha *et al.*<sup>12</sup> Harrison's<sup>13</sup> model potential and Animalu's transition-metal pseudopotential<sup>14</sup> are used for the bare ion potential.

The plan of the paper is as follows. The inversion of the dielectric matrix and the evaluation of the dynamical matrix are presented in Sec. II. The results and calculations are given in Sec. III, and these are discussed in Sec. IV.

### II. THEORY

#### A. Inversion of dielectric matrix

In the noninteracting band scheme the dielectric matrix is written<sup>11</sup>

$$\begin{aligned} \epsilon(\vec{q} + \vec{G}, \vec{q} + \vec{G}') &= \sum_{\sigma} \{ [1 - \epsilon_{ss}^{\sigma}(\vec{q} + \vec{G}, \vec{q} + \vec{G}')] \delta_{GG'} \\ &\quad - \epsilon_{dd}^{\sigma}(\vec{q} + \vec{G}, \vec{q} + \vec{G}') \\ &\quad - \epsilon_{ds}^{\sigma}(\vec{q} + \vec{G}, \vec{q} + \vec{G}') - \epsilon_{sd}^{\sigma}(\vec{q} + \vec{G}, \vec{q} + \vec{G}') \}, \end{aligned} \quad (1a)$$

$$\begin{aligned} \epsilon(\vec{q} + \vec{G}, \vec{q} + \vec{G}') &= \epsilon_0(\vec{q} + \vec{G}) \delta_{GG'} - \epsilon_{dd}(\vec{q} + \vec{G}, \vec{q} + \vec{G}') \\ &\quad - \epsilon_{ds}(\vec{q} + \vec{G}, \vec{q} + \vec{G}') - \epsilon_{sd}(\vec{q} + \vec{G}, \vec{q} + \vec{G}'). \end{aligned} \quad (1b)$$

Here  $\vec{q}$  is the phonon wave vector,  $\vec{G}$  and  $\vec{G}'$  are the reciprocal-lattice vectors,  $\epsilon_0(\vec{q} + \vec{G})$  is the free-electron part of the dielectric function and is a scalar,  $\epsilon_{dd}$  arises due to intra- and inter- $d$ -subbands, transitions, and  $\epsilon_{ds}$  and  $\epsilon_{sd}$  arise owing to interband transitions from  $d$  subbands to the  $s$  band and from the  $s$  band to partially filled  $d$ -subbands, respectively.  $\sum_{\sigma}$  represents the sum for both the majority- and minority-spin bands. Explicitly,  $\epsilon_{dd}(\vec{q} + \vec{G}, \vec{q} + \vec{G}')$  is given as<sup>11</sup>

$$\begin{aligned} \epsilon_{dd}(\vec{q} + \vec{G}, \vec{q} + \vec{G}') &= \nu(\vec{q} + \vec{G}) \sum_{\sigma} \sum_m \sum_m \\ &\quad \times \Delta_{dm, dm'}^{\sigma}(\vec{q} + \vec{G}) f^{\sigma}(\vec{q}) \Delta_{dm', dm}^{\sigma*}(\vec{q} + \vec{G}'). \end{aligned} \quad (2)$$

In the evaluation of Eq. (2), the overlap between

the  $d$  orbitals on different lattice sites which involves the multicentral integrals is assumed to be negligible and only the overlap between the  $d$  orbitals on the same site is explicitly included.  $\nu(\vec{q}+\vec{G})$  is the Fourier transform of the effective electron-electron potential,  $m$  and  $m'$  are magnetic quantum numbers. The analytical expressions for  $\Delta_{dm, dm'}^{\sigma}$   $\times (\vec{q}+\vec{G})$  are the same as given in I and

$$f^{\sigma}(\vec{q}) = - \sum_k \frac{n_{dm\sigma}(\vec{k}) - n_{dm'\sigma}(\vec{k}')}{E_{dm\sigma}(\vec{k}) - E_{dm'\sigma}(\vec{k}')} . \quad (3)$$

$n_{dm\sigma}(\vec{k})$  is the Fermi occupation probability function and  $E_{dm\sigma}(\vec{k})$  is the energy eigenvalue for the Bloch state  $\vec{k}$ .  $\vec{k}' = \vec{k} + \vec{q}$  and lies in the first Brillouin zone. It is evident from Eq. (2) that  $\epsilon_{dd}(\vec{q}+\vec{G}, \vec{q}+\vec{G}')$  is in the separable form.

Since we have used the same radial wave functions for up- and down-spin electrons in I, the overlap integrals  $\Delta_{dm, dm'}^{\sigma}(\vec{q}+\vec{G})$  reduce to be the same for both spins. If we give equal weightage to all the five  $d$  subbands, we get  $\Delta_{dm, dm'}(\vec{q}+\vec{G}) = A(\vec{q}+\vec{G})$ , where

$$A(\vec{q}+\vec{G}) = \int j_0(|\vec{q}+\vec{G}|r) R_{3d}^2(r) r^2 dr , \quad (4)$$

where  $R_{3d}(r)$  is the radial wave function for  $3d$  atomic orbitals and  $j_0(|\vec{q}+\vec{G}|r)$  is the spherical Bessel function of zero order. A similar averaging has also been done by Hanke<sup>9</sup> and Brown.<sup>15</sup> Therefore, we write the intraband part of  $\epsilon_{dd}(\vec{q}+\vec{G}, \vec{q}+\vec{G}')$  as

$$\epsilon_{dd}^{\text{intra}}(\vec{q}+\vec{G}, \vec{q}+\vec{G}') = \nu(\vec{q}+\vec{G}) A(\vec{q}+\vec{G}) f(\vec{q}) A^*(\vec{q}+\vec{G}') . \quad (5)$$

The  $m$  dependence is left only in the band-structure part  $f(q)$  which is explicitly given as

$$f(\vec{q}) = - \frac{N\Omega_0}{4\pi^2 \hbar^2} \sum_{\sigma} \sum_m m_{dm\sigma} k_{Fdm\sigma} \times \left( 1 + \frac{4k_{Fdm\sigma}^2 - q^2}{4k_{Fdm\sigma}q} \ln \left| \frac{2k_{Fdm\sigma} + q}{2k_{Fdm\sigma} - q} \right| \right) . \quad (6)$$

Here  $m_{dm\sigma}$  and  $k_{Fdm\sigma}$  are the effective mass and Fermi momentum for the electron in the  $m$ th  $d$  subband of spin  $\sigma$ .  $N$  is the number of atoms in the crystal and  $\Omega_0$  is the atomic volume.

The expressions for  $\epsilon_{ds}(\vec{q}+\vec{G}, \vec{q}+\vec{G}')$  and  $\epsilon_{sd}(\vec{q}+\vec{G}, \vec{q}+\vec{G}')$  evaluated in paper I are very lengthy and are not presented again here. Because of the nonorthogonality of  $s$  and  $d$  wave functions the interband con-

tributions  $\epsilon_{ds}$  and  $\epsilon_{sd}$  are not in the separable form while the interband part of  $\epsilon_{dd}(\vec{q}+\vec{G}, \vec{q}+\vec{G}')$  is in the separable form. We follow the factorization *Ansatz* due to Sinha *et al.* and give the sum of the interband parts of  $\epsilon_{dd}$ ,  $\epsilon_{ds}$ , and  $\epsilon_{sd}$  in a separable form as

$$\epsilon_{dd}^{\text{inter}} + \epsilon_{ds} + \epsilon_{sd} = \nu(\vec{q}+\vec{G}) B(\vec{q}+\vec{G}) F(\vec{q}) B^*(\vec{q}+\vec{G}') , \quad (7)$$

where the functions  $B(\vec{q}+\vec{G})$  and  $F(\vec{q})$  will be determined with the help of detailed calculations of the total interband part of the dielectric function.

Substituting (5) and (7) in (1b), we can write the dielectric matrix

$$\begin{aligned} \epsilon(\vec{q}+\vec{G}, \vec{q}+\vec{G}') &= \epsilon_0(\vec{q}+\vec{G}) \delta_{GG'} \\ &- \nu(\vec{q}+\vec{G}) A(\vec{q}+\vec{G}) f(\vec{q}) A^*(\vec{q}+\vec{G}') \\ &- \nu(\vec{q}+\vec{G}) B(\vec{q}+\vec{G}) F(\vec{q}) B^*(\vec{q}+\vec{G}') . \end{aligned} \quad (8)$$

Using the orthogonality condition for  $\epsilon(\vec{q}+\vec{G}, \vec{q}+\vec{G}')$  and making some mathematical manipulations which are lengthy but straightforward, we obtain the inverse of the dielectric matrix:

$$\begin{aligned} \epsilon^{-1}(\vec{q}+\vec{G}, \vec{q}+\vec{G}') &= \epsilon_0^{-1}(\vec{q}+\vec{G}') \{ \delta_{GG'} + \nu(\vec{q}+\vec{G}) \\ &\times \epsilon_0^{-1}(\vec{q}+\vec{G}) [ A(\vec{q}+\vec{G}) T(\vec{q}) A^*(\vec{q}+\vec{G}') \\ &- A(\vec{q}+\vec{G}) L^{\dagger}(\vec{q}) B^*(\vec{q}+\vec{G}') \\ &- B(\vec{q}+\vec{G}) L(\vec{q}) A^*(\vec{q}+\vec{G}') \\ &+ B(\vec{q}+\vec{G}) S(\vec{q}) B^*(\vec{q}+\vec{G}') ] \} , \end{aligned} \quad (9)$$

where

$$L(\vec{q}) = - E(\vec{q}) X^{\dagger}(\vec{q}) T(\vec{q}) , \quad (10)$$

$$T(\vec{q}) = [ C^{-1}(\vec{q}) - X(\vec{q}) E(\vec{q}) X^{\dagger}(\vec{q}) ]^{-1} , \quad (11)$$

$$S(\vec{q}) = [ E^{-1}(\vec{q}) - X^{\dagger}(\vec{q}) C(\vec{q}) X(\vec{q}) ]^{-1} , \quad (12)$$

$$V(\vec{q}) = \sum_G B^*(\vec{q}+\vec{G}) \frac{\nu(\vec{q}+\vec{G})}{\epsilon_0(\vec{q}+\vec{G})} B(\vec{q}+\vec{G}) , \quad (13)$$

$$U(\vec{q}) = \sum_G A^*(\vec{q}+\vec{G}) \frac{\nu(\vec{q}+\vec{G})}{\epsilon_0(\vec{q}+\vec{G})} A(\vec{q}+\vec{G}) , \quad (14)$$

$$X(\vec{q}) = \sum_G A^*(\vec{q}+\vec{G}) \frac{\nu(\vec{q}+\vec{G})}{\epsilon_0(\vec{q}+\vec{G})} B(\vec{q}+\vec{G}) . \quad (15)$$

Here the sum runs over all the reciprocal-lattice vectors of the lattice.  $E(\vec{q})$  and  $C(\vec{q})$  are the inverse of the scalar functions  $[F^{-1}(\vec{q}) - V(\vec{q})]$  and  $[f^{-1}(\vec{q}) - U(\vec{q})]$ , respectively.

With the help of Eq. (9), we can easily write down the density response function

$$\begin{aligned} \chi(\vec{q}+\vec{G}, \vec{q}+\vec{G}') &= - \nu^{-1}(\vec{q}+\vec{G}) [ \delta_{GG'} - \epsilon^{-1}(\vec{q}+\vec{G}, \vec{q}+\vec{G}') ] \\ &= - \nu^{-1}(\vec{q}+\vec{G}) [ 1 - \epsilon_0^{-1}(\vec{q}+\vec{G}) ] \delta_{GG'} \\ &+ \left( \frac{A(\vec{q}+\vec{G})}{\epsilon_0(\vec{q}+\vec{G})} T(\vec{q}) \frac{A^*(\vec{q}+\vec{G}')}{\epsilon_0(\vec{q}+\vec{G}')} - \frac{A(\vec{q}+\vec{G})}{\epsilon_0(\vec{q}+\vec{G})} L^{\dagger}(\vec{q}) \frac{B^*(\vec{q}+\vec{G}')}{\epsilon_0(\vec{q}+\vec{G}')} \right. \\ &\left. - \frac{B(\vec{q}+\vec{G})}{\epsilon_0(\vec{q}+\vec{G})} L(\vec{q}) \frac{A^*(\vec{q}+\vec{G}')}{\epsilon_0(\vec{q}+\vec{G}')} + \frac{B(\vec{q}+\vec{G})}{\epsilon_0(\vec{q}+\vec{G})} S(\vec{q}) \frac{B^*(\vec{q}+\vec{G}')}{\epsilon_0(\vec{q}+\vec{G}')} \right) . \end{aligned} \quad (16)$$

Here the electron-density response function splits into two parts—a purely diagonal part analogous to that of the free-electron gas except that the free-electron dielectric function is replaced by  $\epsilon_0(\vec{q} + \vec{G})$ , and a part which corresponds to a set of dipole and monopole distributions centered at the ion sites and characterized by the screened form factors  $B(\vec{q} + \vec{G})/\epsilon_0(\vec{q} + \vec{G})$  and  $A(\vec{q} + \vec{G})/\epsilon_0(\vec{q} + \vec{G})$ , respectively.  $V$  and  $U$  given by Eqs. (13) and (14) can be regarded as the coupling coefficients between dipolar and monopolar distributions which interact via a screened effective electron-electron interaction  $\nu(\vec{q} + \vec{G})/\epsilon_0(\vec{q} + \vec{G})$ . Therefore,  $\epsilon_0(\vec{q} + \vec{G})$  acts as a screening function for the rest of the interactions. Here what has been termed as the purely diagonal part  $\epsilon_0(\vec{q} + \vec{G})$ , is not the only total diagonal contribution to  $\epsilon(\vec{q} + \vec{G}, \vec{q} + \vec{G})$ , because the diagonal part is also included in  $d$ - $d$  intraband and  $d$ - $d$ ,  $d$ - $s$ , and  $s$ - $d$  interband parts.

The physical meanings of the functions  $\epsilon^{-1}(\vec{q} + \vec{G}, \vec{q} + \vec{G}')$  and  $\chi(\vec{q} + \vec{G}, \vec{q} + \vec{G}')$  can only become transparent in certain limiting cases. For instance, if we neglect  $A(\vec{q} + \vec{G})$  and  $B(\vec{q} + \vec{G})$ , the dielectric function becomes the free-electron dielectric function and conventional screening theory is retrieved. If we put  $B(\vec{q} + \vec{G}) = 0$ , the formulation due to Hanke<sup>9</sup> is obtained. Substituting  $\epsilon_0(\vec{q} + \vec{G}) = 1$  and  $A(\vec{q} + \vec{G})$

= 0, the dipolar model for insulators is obtained. The physical model that results from Eq. (8), consisting of both the dipolar and monopolar distributions associated with  $d$  electrons, is similar to that of the breathing-shell model for insulators.

### B. Lattice dynamics

Assuming that the rigid-ion-core and adiabatic approximations are valid, the phonon frequencies  $\omega_j(\vec{q})$  for the  $j$ th mode can be obtained for a monoatomic lattice in the harmonic approximation by solving the determinantal equation,

$$\det \| D_{\alpha\beta}(\vec{q}) - M\omega_j^2(\vec{q})\delta_{\alpha\beta} \| = 0, \quad (17)$$

where  $D_{\alpha\beta}(\vec{q})$  are the elements of the dynamical matrix,  $\alpha, \beta$  are the Cartesian components, and  $M$  is the mass of the ion. We can write

$$D_{\alpha\beta}(\vec{q}) = \bar{D}_{\alpha\beta}(\vec{q}) - \bar{D}_{\alpha\beta}(0), \quad (18)$$

where

$$D_{\alpha\beta}(\vec{q}) = \frac{4\pi Z^2 e^2}{\Omega_0} \sum_{G'} \frac{(\vec{q} + \vec{G})_\alpha (\vec{q} + \vec{G}')_\beta}{|\vec{q} + \vec{G}'|^2} \epsilon^{-1}(\vec{q} + \vec{G}, \vec{q} + \vec{G}'), \quad (19)$$

$Z$  is the ionicity, and  $e$  is the electronic charge. Substituting Eq. (9) in (19), we have

$$\begin{aligned} \bar{D}_{\alpha\beta}(\vec{q}) = & \frac{4\pi Z^2 e^2}{\Omega_0} \sum_G \frac{(\vec{q} + \vec{G})_\alpha (\vec{q} + \vec{G})_\beta}{|\vec{q} + \vec{G}|^2} + \frac{4\pi Z^2 e^2}{\Omega_0} \sum_G \frac{(\vec{q} + \vec{G})_\alpha (\vec{q} + \vec{G})_\beta}{|\vec{q} + \vec{G}|^2} [\epsilon_0^{-1}(\vec{q} + \vec{G}) - 1] \\ & + N \left( \sum_G (\vec{q} + \vec{G})_\alpha A(\vec{q} + \vec{G}) \frac{W(\vec{q} + \vec{G})}{\epsilon_0(\vec{q} + \vec{G})} \right) T(\vec{q}) \left( \sum_{G'} A^*(\vec{q} + \vec{G}') \frac{W(\vec{q} + \vec{G}')}{\epsilon_0(\vec{q} + \vec{G}')} (\vec{q} + \vec{G}')_\beta \right) \\ & + N \left( \sum_G (\vec{q} + \vec{G})_\alpha B(\vec{q} + \vec{G}) \frac{W(\vec{q} + \vec{G})}{\epsilon_0(\vec{q} + \vec{G})} \right) S(\vec{q}) \left( \sum_{G'} B^*(\vec{q} + \vec{G}') \frac{W(\vec{q} + \vec{G}')}{\epsilon_0(\vec{q} + \vec{G}')} (\vec{q} + \vec{G}')_\beta \right) \\ & - N \left( \sum_G (\vec{q} + \vec{G})_\alpha A(\vec{q} + \vec{G}) \frac{W(\vec{q} + \vec{G})}{\epsilon_0(\vec{q} + \vec{G})} \right) L^\dagger(\vec{q}) \left( \sum_{G'} B^*(\vec{q} + \vec{G}') \frac{W(\vec{q} + \vec{G}')}{\epsilon_0(\vec{q} + \vec{G}')} (\vec{q} + \vec{G}')_\beta \right) \\ & - N \left( \sum_G (\vec{q} + \vec{G})_\alpha B(\vec{q} + \vec{G}) \frac{W(\vec{q} + \vec{G})}{\epsilon_0(\vec{q} + \vec{G})} \right) L(\vec{q}) \left( \sum_{G'} A^*(\vec{q} + \vec{G}') \frac{W(\vec{q} + \vec{G}')}{\epsilon_0(\vec{q} + \vec{G}')} (\vec{q} + \vec{G}')_\beta \right). \end{aligned} \quad (20)$$

Here  $W(\vec{q} + \vec{G})$  is the Fourier transform of bare ion potential. The first term of Eq. (20) represents the contribution from the direct ion-ion Coulomb interaction, which can be evaluated by Ewald's  $\theta$ -function transformation. The second term in Eq. (20) is the simple metal ion-electron-ion interaction term. The third and fourth terms arise due to monopole-monopole and dipole-dipole interactions, respectively. The last two terms are due to interactions between dipoles and monopoles.

## III. CALCULATIONS AND RESULTS

### A. Paramagnetic nickel

The diagonal and the nondiagonal parts of the dielectric matrix are calculated for paramagnetic

nickel using the formalism of paper I, where the spin index  $\sigma$  is removed and the expressions are multiplied by a factor of 2 for spin degeneracy. The total interband part of the dielectric function is expressed by Eq. (7). The functions  $B(\vec{q} + \vec{G})$  and  $F(\vec{q})$  are obtained by the method of least-squares fit and are given as

$$B(\vec{q} + \vec{G}) = \begin{cases} 0.3911 |\vec{q} + \vec{G}| \exp(69.254 |\vec{q} + \vec{G}|) \\ -302.441 |\vec{q} + \vec{G}|^2 \text{ for } |\vec{q} + \vec{G}| \leq 0.2, \\ 1.6731 |\vec{q} + \vec{G}| \exp(-0.6457 |\vec{q} + \vec{G}|) \\ \text{for } |\vec{q} + \vec{G}| > 0.2, \end{cases} \quad (21)$$

and

$$F(\vec{q}) = -N/q. \quad (22)$$

All the parameters used in the calculation of the dielectric matrix for paramagnetic nickel are the same as given in the paper of Prakash and Joshi<sup>7</sup> for the configuration  $3d^3.4s^0.6$ .

In view of the difficulties discussed in Ref. 7 we replace the bare ion potential by the Harrison model potential, which is given as

$$U_b(\vec{q}) = -4\pi Ze^2/q^2 + \beta_c [1 + (q\gamma_c)^2]^{-2}. \quad (23)$$

The first term represents the Coulomb potential due to the ionic charge  $Ze$  while the second term represents the repulsive part of the potential.  $\beta_c$  is the strength of this repulsion and the parameter  $\gamma_c$  is introduced to bring the desired decay of  $U_b(\vec{q})$  for large  $\vec{q}$ . The parameters  $\beta_c$  and  $\gamma_c$  are adjusted to achieve the rapid convergence in the sum over reciprocal-lattice vectors and to force an agreement between the calculated and experimental phonon frequencies. This model potential is a good approximation for  $s$ -like electrons. Hanke pointed out that the potential seen by  $d$  electrons should be purely Coulombic because of the tight-binding wave functions used for  $d$  electrons. However, in principle, the  $d$  electrons are not completely localized, and the potential seen by  $d$  electrons deviates from central field, which is explicitly pointed out by Animalu<sup>14</sup> in his calculations based on a transition-metal model potential (TMMP). Noncentral forces for  $d$  electrons are again an essential feature of the Harrison transition-metal pseudopotential,<sup>2</sup> and this gives rise to the hybridization term distinguishing the simple metals and  $d$ -band transition metals. However, the noncentral potentials for  $s$  and  $d$  electrons may be of different nature, but in view of the computational difficulties and parametrized nature of the model potential, we use the same potential for  $s$  and  $d$  electrons in the calculation of phonon frequencies.

The effective electron-electron interaction including exchange and correlation corrections is written

$$v(\vec{q}) = (4\pi e^2/N\Omega_0 q^2) [1 - f_{xc}(\vec{q})]. \quad (24)$$

For  $s$  electrons we use the Singwi *et al.*<sup>16</sup> Gaussian functional form

$$f_{xc}(\vec{q}) = A' \{1 - \exp[-B'(q|k_{Fss})^2]\}, \quad (25)$$

where the parameters  $A'$  and  $B'$  are chosen from consideration of interelectronic distances of  $s$  electrons. Equation (25) is obtained for free electrons and, therefore, hardly justified for  $d$  electrons because of their tight-binding nature. Moreover an explicit functional form for exchange and correlation corrections for  $d$  electrons is not yet established. Moriarty<sup>3</sup> in his first-principles calculations of phonon frequencies and binding energies of noble metals used the free-electron exchange ap-

proximation for core-conduction exchange for  $d$  electrons in a manner suggested by Lindgren<sup>17</sup> and concluded that the core-conduction exchange correction for  $d$  electrons is very important, as its inclusion removes the hump in the form factors in the low- $\vec{q}$  region. A similar approximation for core-conduction exchange is also used by Panitz, King, and Cutler<sup>5</sup> in the calculation of phonon frequencies of zinc. However, in view of the parametrized nature of the model potential, we treat the  $d$  electrons in the Hartree approximation and neglect the core-conduction exchange and exchange-correlation corrections for  $d$  electrons. The core-conduction exchange for  $s$  electrons is also assumed to be very small as in free-electron metals.<sup>13</sup>

The phonon frequencies for paramagnetic nickel are calculated using the parameters  $\beta_c = 16.0$  and  $\gamma_c = 0.3$  which were used by Prakash and Joshi. These results are shown in Fig. 1 by dash-double-dot lines. We find that agreement with experimental values<sup>18</sup> is improved for the transverse branches while the results for longitudinal branches are larger than the experimental values. However, the parameters in the paper of Prakash and Joshi were obtained by a forced fit with the experimental values where only the intraband diagonal part of the dielectric function was included. In the present scheme, we are including the nondiagonal intraband and diagonal and nondiagonal interband parts of the dielectric matrix which give rise to local field corrections and also include the exchange and correlation corrections for  $s$  electrons. In view of the fact that the present scheme includes an improved dielectric function, we again readjust the parameters  $\beta_c$  and  $\gamma_c$  by fitting the phonon frequencies at  $q = (2\pi/a)(0.2, 0.0, 0.0)$  and at  $q = (2\pi/a)(0.1, 0.1, 0.1)$  in the longitudinal branches in the [100] and [111] directions, respectively, which is equivalent to obtaining a good fit for the elastic constants as done by Hanke.<sup>9</sup> The values of the parameters  $\beta_c$  and  $\gamma_c$  are 3.2 and 0.3, respectively. The calculations are repeated for all the branches in all the three principal symmetry directions. These results are also shown in the Fig. 1 by solid lines.

Very recently, Animalu has suggested the transition-metal model (TMMP) which includes  $s$ - $d$  hybridization, while this hybridization was not explicitly included in the Harrison model potential. Animalu calculated the phonon frequencies of paramagnetic nickel, neglecting the ion-ion overlap contribution and using the free-electron dielectric function. However, the TMMP parameters tabulated by Animalu are not the absolute parameters. These have been obtained by fitting the phonon frequencies at the  $X$  point in the longitudinal branch. Because these parameters are obtained in conjunction with the free-electron dielectric function, which is hardly justified for transition metals, do

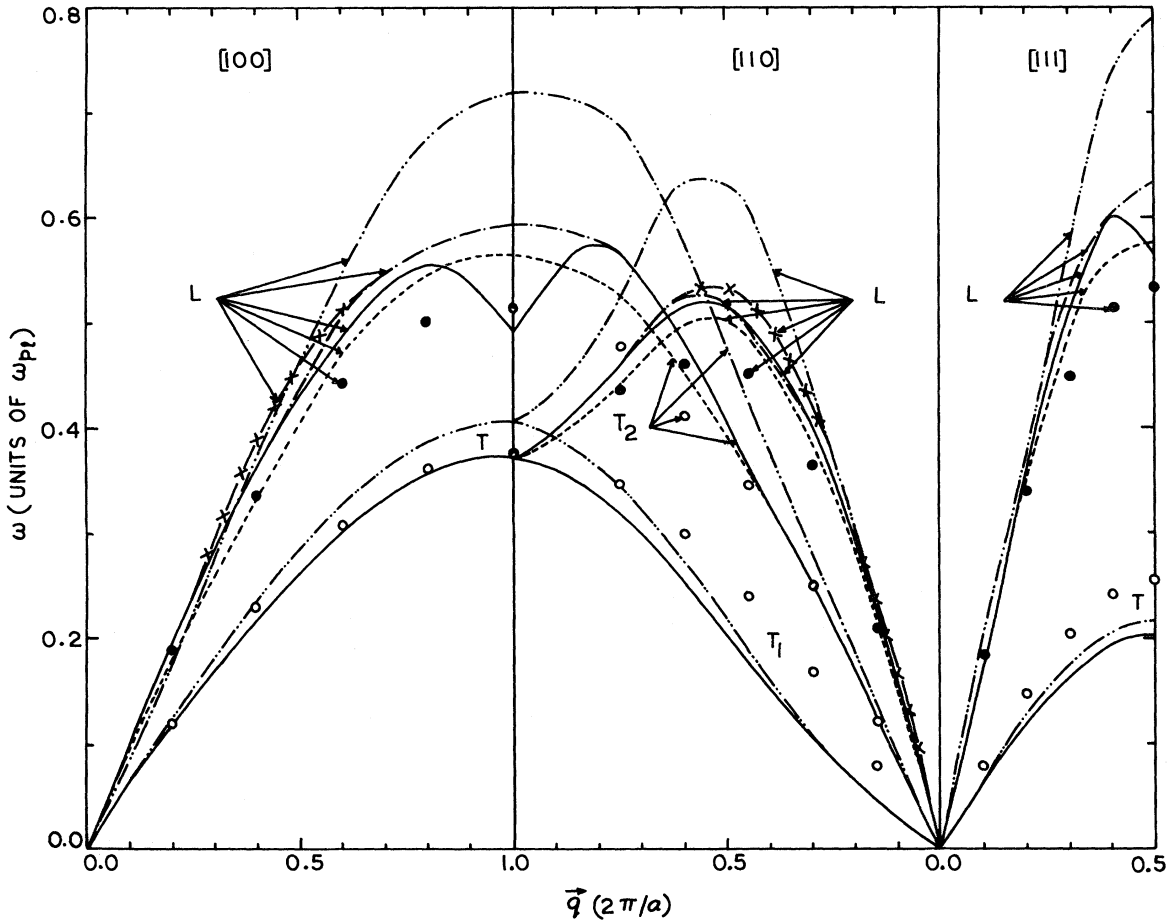


FIG. 1.  $\omega(\vec{q})$  vs  $\vec{q}$  for paramagnetic nickel. Solid and dash-double-dot lines show the phonon frequencies with the parameters  $(\beta_c, \gamma_c)$  as  $(3.2, 0.3)$  and  $(16.0, 0.3)$ , respectively. Dash-dot and dash-cross lines represent the phonon frequencies with the parameters  $\beta_c=3.2$  and  $\gamma_c=0.3$  with the interband part of the dielectric matrix excluded and in the free-electron limit, respectively. Dashed lines show the phonon frequencies using Animalu's TMMP. For the transverse branches the solid and dashed lines coincide. Solid and open circles show experimental points in the longitudinal and transverse branches, respectively.  $a$  is lattice constant and  $\omega_{p1}$  is the plasma frequency.

not yield a good fit with experimental values while we use our dielectric function, which is definitely an improvement over the free-electron dielectric function. Therefore, we renormalize the parameters of Animalu's TMMP to get the best agreement with the experimental values. The renormalized parameters  $A_0$ ,  $A_1$ ,  $R_m$ , and  $\alpha_{eff}$  in our calculations are 1.4, 1.4, 2.35, and 0.0, respectively, and the remaining parameters are the same as tabulated by Animalu. The results for this calculation are also shown in Fig. 1 by dashed lines.

#### B. Ferromagnetic nickel

In Paper I, we calculated the diagonal and non-diagonal parts of the dielectric matrix in the non-interacting-spin band model in the Hartree approximation for ferromagnetic nickel. The total dielectric function is obtained by summing up the contri-

butions of all the intra- and interband transitions in the up- and down-spin bands. The expressions for the free-electron part and the intraband part are retained from Paper I while we represent the total interband part in separable form as given in Eq. (7). The function  $B(\vec{q}+\vec{G})$ , obtained by the method of least-squares fit is

$$B(\vec{q}+\vec{G}) = \begin{cases} 362.60 |\vec{q}+\vec{G}| \\ \times \exp(-72.10566 |\vec{q}+\vec{G}| + 142.60709) \\ \times |\vec{q}+\vec{G}|^2 \text{ for } |\vec{q}+\vec{G}| \leq 0.2, \\ 3.062 |\vec{q}+\vec{G}|^2 \exp(-|\vec{q}+\vec{G}|^2) \\ \text{for } |\vec{q}+\vec{G}| > 0.2. \end{cases} \quad (26)$$

The function  $F(\vec{q})$  is the same as given in Eq. (22). The exchange-correlation corrections are used in the same manner as in the paramagnetic phase.

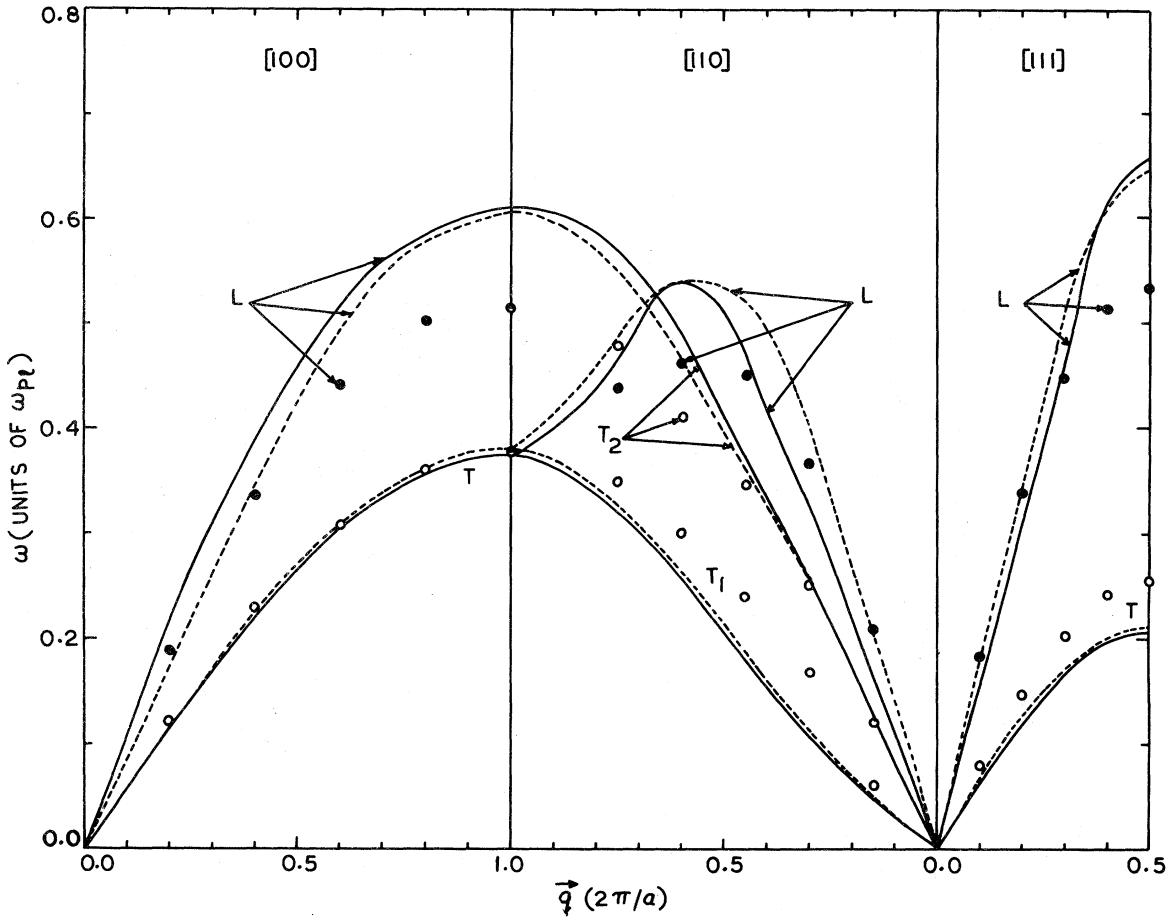


FIG. 2.  $\omega(\vec{q})$  vs  $\vec{q}$  for ferromagnetic nickel. Solid lines show the phonon frequencies using Harrison's model potential for  $\beta_c=3.2$  and  $\gamma_c=0.3$ . Dashed lines represent the phonon frequencies using Animalu's TMMP with the same parameters as for the paramagnetic phase.

We calculated the phonon frequencies for ferromagnetic nickel along the three principal symmetry directions for all the longitudinal and transverse branches using the same parameters as for paramagnetic nickel for the Harrison simple-metal model potential. These results are shown by solid lines in Fig. 2 along with experimental results of Birgeneau *et al.*<sup>18</sup> for the ferromagnetic phase. We also tried to readjust the parameters  $\beta_c$  and  $\gamma_c$  to get the best fit for the ferromagnetic phase. However, no appreciable improvement was found in the results and therefore these are not shown in Fig. 2. Further forced fit with the experimental values was avoided at this stage of calculation. We also used the Animalu TMMP in conjunction with our dielectric function for the ferromagnetic phase to calculate the phonon frequencies. These results are also shown by the dashed lines in the Fig. 2.

In this calculation of phonon frequencies of ferromagnetic nickel, the same model potential has been used for the up- and down-spin electrons which seems to be rather unrealistic. In the isotropic

noninteracting band model, the up- and down-spin  $s$  bands coincide with each other while the down-spin  $d$  subbands are shifted with respect to up-spin  $d$  subbands by 0.05 Ry, which is approximately 20% of the bandwidth. This certainly demands the separate bare ion potential for up- and down-spin  $d$  electrons. This may be incorporated in the present scheme but it demands heavy computational efforts and it will again lead us to the parametrized form of the potential. A rigorous justification can be made only if the first-principles calculation of the bare ion potential and the exchange-correlation corrections are carried out. It has been pointed out by Hayashi and Shimizu<sup>19</sup> that the exchange splitting for ferromagnetic nickel is small and does not contribute appreciably for impurity screening. Also in view of the computational difficulties and the other approximations for  $d$  electrons discussed for the paramagnetic phase, this simplification may not be too serious for a calculation of phonon frequencies of ferromagnetic nickel to lowest order. Therefore, this detailed analysis remains purely

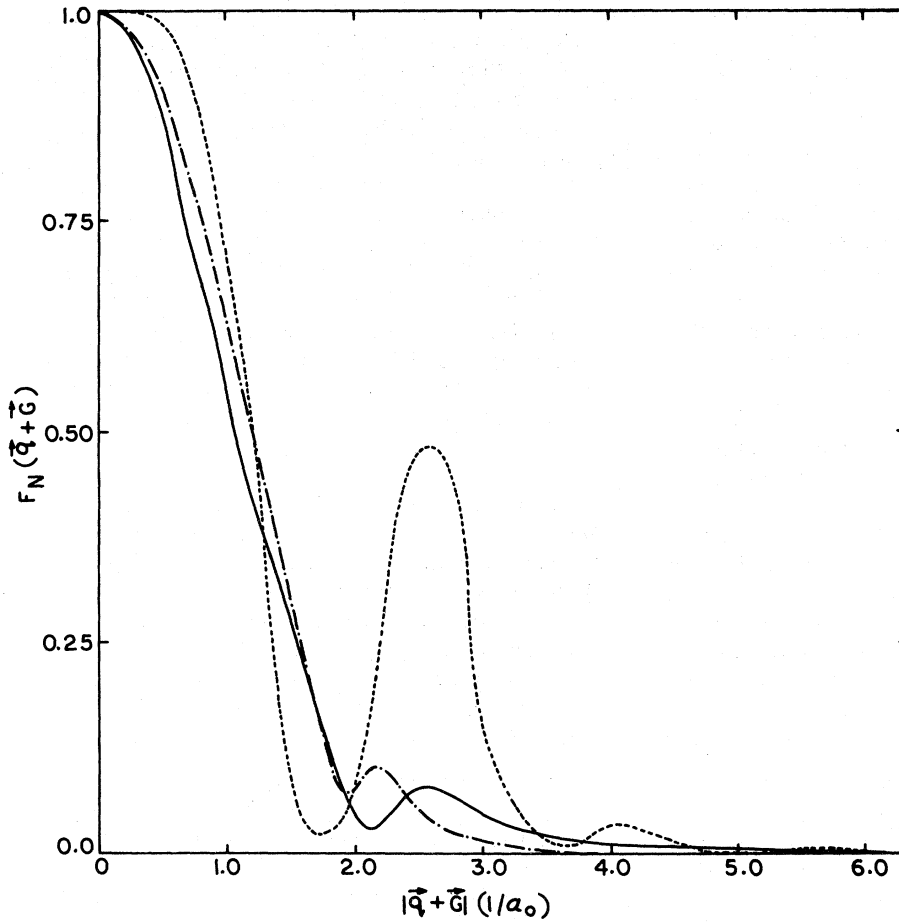


FIG. 3.  $F_N(\vec{q} + \vec{G})$  vs  $|\vec{q} + \vec{G}|$ . Solid and dash-dot lines represent the normalized energy wave-number characteristics of the paramagnetic and ferromagnetic phases, respectively, for the same parameters  $\beta_c$  and  $\gamma_c$ . Dash-dot lines show the energy wave-number characteristic of paramagnetic nickel using Animalu's model potential.  $a_0$  is Bohr's radius.

academic.

The normalized energy wave-number characteristic function is defined

$$F_N(\vec{q}) = [1 - \epsilon^{-1}(\vec{q})] \left( -1 + \frac{q^2}{4\pi Z e^2} \frac{\beta_c}{[1 + (q\gamma_c)^2]^2} \right)^2, \quad (27)$$

where  $\epsilon(\vec{q})$  is the total diagonal part of the dielectric function.  $F_N(\vec{q})$  is calculated for both paramagnetic and ferromagnetic nickel using the Harrison model potential with the same parameters.  $F_N(\vec{q})$  is also calculated for paramagnetic nickel using Animalu's potential. These results are shown in Fig. 3. The  $F_N(\vec{q})$  calculated for other cases of the ferromagnetic phase are similar and not shown in the diagram for neatness.

#### IV. DISCUSSION

In the case of paramagnetic nickel the transverse branches are in better agreement with the experimental values except near the zone boundary in the [111] direction and for intermediate values of  $\vec{q}$  in the [110] direction, when the interband part is included in the dielectric function and Harrison's model potential is used. The calculated phonon frequencies for the longitudinal branches are

larger than the experimental results for large values of  $\vec{q}$ . Softening of the longitudinal modes near the zone boundary is also found. However in our calculations such a softening is not found in the transverse branches. The experimental phonon frequencies for fcc transition metals do not show such softening while it is found for bcc transition metals.

If the interband part of the dielectric matrix is switched off, the phonon frequencies in the longitudinal branches are enhanced about 20% near the zone boundary. The softening of the longitudinal modes also disappears. The phonon frequencies of transverse branches remain unaffected. In the free-electron limit, the phonon frequencies of the longitudinal branches are further enhanced, while the frequencies in the transverse branches remain almost unaffected.

In the phonon frequencies calculated using Animalu's model potential, the softening of the longitudinal modes near the zone boundary disappears. The agreement between the theoretical and the experimental values improves at the maximum by 5% in the longitudinal branches while the transverse branches show a good agreement with the experimental values. The results may further be improved

by including core-conduction exchange and exchange-correlation corrections for  $d$  electrons.

In the ferromagnetic phase the transverse branches are in reasonably good agreement with the experimental values. The longitudinal branches show a good agreement in the low- $\vec{q}$  region while the calculated phonon frequencies using the Harrison model potential are large, as compared with the experimental values, near the zone boundary. But the calculated phonon frequencies using the TMMP are in better agreement in all branches for all values of  $\vec{q}$ . Comparing with the paramagnetic phase the phonon frequencies in the ferromagnetic phase are enhanced by about 5%, which is consistent with the neutron spectroscopic results of deWit and Brockhouse.<sup>20</sup> Our calculations for the ferromagnetic phase are rather preliminary. We use an oversimplified picture of a very complicated system of ferromagnetic nickel. The exchange and correlation potentials which are very important in the ferromagnetic phase should be included consistently in the evaluation of the dielectric function as well as in the bare ion potential. However, actual calculations of phonon frequencies using such a scheme will be a prohibitively difficult task.

The energy wave-number characteristic function

shows the usual behavior for both the paramagnetic and ferromagnetic phases. This converges in the limit of sum over  $\vec{G}$  for 363 reciprocal-lattice vectors. The  $F_N(\vec{q})$  due to Animalu's potential shows oscillatory nature because this model potential consists of sine and cosine terms. The qualitative behavior of all the curves is the same.

In conclusion, we examined here a model for lattice dynamics of transition metals similar to that of the screened-breathing-shell model for insulators using the factorization *Ansatz* due to Sinha *et al.* Our calculation of phonon frequencies for ferromagnetic nickel can be regarded only as the first step towards the solution of a characteristically difficult problem.

#### ACKNOWLEDGMENTS

The authors are thankful to Professor S. K. Joshi, Professor S. K. Sinha, and Dr. K. N. Pathak for very helpful discussions, and to Professor H. S. Hans for encouragement. The authors are indebted to Professor S. K. Sinha for sending the preprints of his papers much before publication. The financial assistance from Council of Scientific and Industrial Research, New Delhi, and University Grants Commission is also acknowledged.

- 
- <sup>1</sup>L. F. Mattheiss, Phys. Rev. **134**, A970 (1964); J. Yamashita, M. Fukuchi, and W. Wakoh, J. Phys. Soc. Jpn. **18**, 999 (1963); **19**, 1342 (1964); S. Wakoh, *ibid.* **20**, 1894 (1965); L. Hodges, E. Ehrenreich, and N. D. Lang, Phys. Rev. **152**, 505 (1966); J. W. D. Connolly, *ibid.* **159**, 415 (1967); J. Callway and C. S. Wang, Phys. Rev. B **7**, 1096 (1973).
- <sup>2</sup>W. A. Harrison, Phys. Rev. **181**, 1036 (1969).
- <sup>3</sup>J. A. Moriarty, Phys. Rev. B **1**, 1362 (1970); **6**, 1239 (1972); **6**, 2066 (1972).
- <sup>4</sup>J. Panitz, P. H. Cutler, and W. H. King, J. Phys. F **4**, L106 (1974).
- <sup>5</sup>S. K. Sinha, Phys. Rev. **169**, 477 (1968).
- <sup>6</sup>D. C. Golibersuch, Phys. Rev. **157**, 532 (1967).
- <sup>7</sup>S. Prakash and S. K. Joshi, Phys. Rev. B **2**, 915 (1970); **4**, 1770 (1971); **5**, 2880 (1972).
- <sup>8</sup>N. Singh and S. Prakash, Phys. Rev. B **8**, 5532 (1973).
- <sup>9</sup>W. Hanke, Phys. Rev. B **8**, 4585 (1973).
- <sup>10</sup>J. Singh, N. Singh, and S. Prakash (unpublished).
- <sup>11</sup>N. Singh, J. Singh, and S. Prakash, Phys. Rev. B **12**, 1076 (1975).
- <sup>12</sup>S. K. Sinha, R. P. Gupta, and D. L. Price, Phys. Rev. B **9**, 2564 (1974).
- <sup>13</sup>W. A. Harrison, *Pseudopotential in the Theory of Metals* (Benjamin, New York, 1966), p. 298.
- <sup>14</sup>A. O. E. Animalu, Phys. Rev. B **8**, 3542 (1973).
- <sup>15</sup>J. S. Borwn, J. Phys. F **2**, 115 (1972).
- <sup>16</sup>K. S. Singwi, A. Sjölander, M. P. Tosi, and R. H. Land, Phys. Rev. B **1**, 1044 (1970); **2**, 2983 (1970).
- <sup>17</sup>I. Lindgren, Int. J. Quantum Chem. **5**, 411 (1971).
- <sup>18</sup>R. J. Birgeneau, J. Cords, G. Dolling, and A. D. W. Woods, Phys. Rev. **136**, A1359 (1964).
- <sup>19</sup>E. Hayashi and M. Shimizu, J. Phys. Soc. Jpn. **26**, 1396 (1969); **27**, 43 (1969).
- <sup>20</sup>G. A. deWit and B. N. Brockhouse, J. Appl. Phys. **39**, 451 (1968).